Energy & Environmental Science

Optimal Energy Storage Portfolio for High and Ultrahigh Carbon-Free and Renewable Power Systems

Journal:	*Energy & Environmental Science*
Manuscript ID	EE-ANA-06-2021-001835.R2
Article Type:	Analysis
Date Submitted by the Author:	23-Aug-2021
Complete List of Authors:	Guerra, Omar; National Renewable Energy Laboratory, Chemical Engineering Eichman, Joshua; National Renewable Energy Laboratory Denholm, Paul; National Renewable Energy Laboratory

Optimal Energy Storage Portfolio for High and Ultrahigh Carbon-Free and Renewable Power Systems

Omar J. Guerra[1, §], Joshua Eichman[1], and Paul Denholm[1]

[1] National Renewable Energy Laboratory. 15013 Denver West Parkway, Golden, CO 80401, U.S.

[§] e-mail: omarjose.guerrafernandez@nrel.gov

Abstract

Achieving 100% carbon-free or renewable power systems can be facilitated by the deployment of energy storage technologies at all timescales, including short-duration, long-duration, and seasonal scales; however, most current literature focuses on cost assessments of energy storage for a given timescale or type of technology. Here, we use an optimization framework with high spatial and temporal resolution to simultaneously assess the variable renewable power deployment and the optimal storage portfolio for seven independent system operators in the United States. Results indicate that achieving high (75%–90%) and ultrahigh (>90%) energy mixes requires combining several flexibility options, including renewable curtailment, short-duration, long-duration, and seasonal storage. For instance, carbon-free and renewable energy mix targets of up to 80% are achieved with economic curtailment and a combination of short- and long-duration energy storage for the performance and cost assumptions used. After that, there is a point between 80% and 95% where seasonal storage becomes cost-competitive, depending on the specific power system. Moreover, our results indicate that storage-to-storage operation—one storage device used to charge another storage device—and the decoupling of charging and discharging storage power capacity are cost-effective options for the integration of high and ultrahigh shares of carbon-free or renewable power sources. Additionally, the results from this study show that an 85% carbon-free or renewable energy mix can be achieved at a cost of avoided CO_2 emissions of US$66.0 per tonne or less, regardless of the power system.

Power systems are undergoing rapid changes driven by national and regional energy policies, falling costs of wind and solar photovoltaic (PV) power, and the electrification of energy demand, among other factors[1]. Achieving high and ultrahigh clean or renewable energy systems poses significant technical and operational challenges to planning and operations[2,3]. The large-scale integration of variable renewable energy (VRE) requires enhancing power system flexibility to accommodate steeper and/or more frequent fluctuations in net load—electricity load minus VRE availability. A broad range of approaches could provide power system flexibility, including operational strategies (e.g., VRE curtailment, demand-side management), energy storage, spatial diversity of generation resources (including transmission expansion), and sector coupling[1,4]. Note that this paper

defines high levels of clean or renewable energy shares between 75% and 90% on an annual energy basis across the power system. Additionally, ultrahigh levels of clean or renewable energy correspond to energy shares >90%.

Energy storage could help address VRE integration issues across timescales[5–7]. For example, subhourly and diurnal shifts of VRE generation can be addressed by storage with less than 10 hours of discharge duration, including flywheels and many battery types[8,9]. Longer-duration discharge (>10 hours and <100 hours)[10,11] storage—such as compressed air energy storage (CAES), pumped hydro storage (PHS), and hydrogen—can address inter-day shifts of VRE power output[12,13]. Achieving 100% carbon-free or renewable power systems could require shifting VRE generation across weeks or months and enhancing resilience to extreme events. These issues could be addressed by seasonal energy storage (>100 hours of discharge duration), including hydrogen and other fuels and systems[14,15]. The least-cost solutions will likely involve a diverse portfolio of generation and storage technologies, with each contributing to supporting grid operations[16,17].

Although energy storage is widely recognized as a key enabling technology for the integration of VRE[18–20], studies on grid-integrated storage have been limited in scope. Most focus on the storage cost assessment for a given timescale or a type of technology [21–23], market-based opportunities[24–26], or are based on a limited set of technologies [17,27] or a limited spatial scope (e.g., analysis of a single region)[28,29]. There is a need for comprehensive assessments of the optimal storage portfolio—power capacity and duration—in view of high and ultrahigh carbon-free or renewable power systems. The following aspects of VRE integration and storage deployment, in particular, require a better understanding: (i) How does the energy mix affect the optimal energy storage portfolio? (ii) How does the least-cost storage portfolio vary as a function of the VRE share? (iii) What is the optimal portfolio of storage devices in high and ultrahigh carbon-free or renewable power systems? and (iv) What are the economics of large-scale VRE integration and storage deployment in power systems?

Grid planning models often use a reduced temporal representation (e.g., characteristic days) to make investment decisions, but this can present challenges when modeling long-duration and seasonal energy storage if the temporal decomposition does not accurately represent the cumulative interaction between time periods[14]. Here, we use an electric grid planning framework with high spatial and temporal resolution to provide detailed insight into large-scale VRE integration and energy storage deployment in power systems. The planning framework provides a more robust representation of storage operation across different timescales, from short-duration to seasonal, and it takes advantage of the spatiotemporal diversity and complementarity between solar PV and wind generation. We use load, generation mix, and weather data from seven independent system operators (ISOs) in the United States to optimize the large-scale integration of VRE generation and the associated storage portfolio in terms of power and energy capacity.

Electric grid planning framework

To evaluate the optimal energy storage and VRE generation portfolio for high and ultrahigh carbon-free or renewable power systems, we propose the Storage Deployment Optimization Model (SDOM). SDOM is designed to accurately represent the operation of storage across different timescales, including long-duration and seasonal applications, and the spatiotemporal diversity and complementarity among VRE sources. SDOM uses an hourly temporal resolution, a fine spatial resolution for VRE sources, and a 1-year optimization window. The same temporal resolution and optimization window have been used in previous work[27,30] but with a lower spatial resolution[12,30,31]. Thus, SDOM uses a better representation of the spatial variability of VRE generation, land-use constraints for VRE siting, and required transmission capacity for the integration of VRE sources. We assume that all builds of VRE are accompanied by sufficient additional transmission capacity to allow for the full utilization of these additional resources, similar to previous approaches[27,28]. Installed capacity and operational profiles for existing nuclear, hydropower, biomass, and geothermal plants are fixed based on operational data (time series) for a given year; thus, SDOM minimizes total system cost using conventional generators as the balancing unit and using VRE and storage technologies to achieve a user-defined carbon-free or renewable energy target. The total system cost includes capital costs, fixed operation-and-maintenance (FO&M) costs, variable operation-and-maintenance (VO&M) costs, and fuel costs for power generation and storage technologies. An overview of SDOM is presented in Supplementary Fig. 1, and the corresponding mathematical formulation is described in Methods.

The optimization framework is used to evaluate the optimal VRE generation and storage portfolio for seven ISOs. Combined, these ISOs are projected to represent ~65% of total electricity demand in the United States by 2050[32], a projected growth of ~27% from 2019 to 2050[32]. By analyzing multiple regions, this study allows for a more comprehensive analysis of the effects of the energy mix and load shape on the optimal energy storage portfolio. We consider six renewable energy targets: 75%, 80%, 85%, 90%, 95%, and 100% (and the same scenarios for the carbon-free cases). The model maintains existing nuclear, hydropower, biomass and geothermal, and it is allowed to expand wind and solar PV capacity. Wind and solar PV deployment and power capacity are optimized using generation profiles and maximum available capacity from the Renewable Energy Potential (reV) model[33], as described in Methods. Nuclear generation is removed from the generation mix for the renewable energy target scenarios, but it is included for the carbon-free target sensitivity scenario provided in the Supplementary Information.

Table 1 presents summaries of the ISO load and generation, whereas the techno-economic assumptions for VRE, balancing units, and storage technologies are presented in Supplementary Table 1. The VRE reference cost values are used as the base case for costs, whereas the projected minimum and maximum costs are used for a sensitivity analysis. We consider four storage technologies representing different classes of technologies being deployed or under development, with details presented in Supplementary Table 1. Each

technology has independent power and energy costs so the model can optimize duration in addition to total power capacity. Short-duration (SD) storage has high energy-related costs but the lowest power-related costs. Like all technologies, short duration can be built to any duration, but the higher duration-related costs tend to make shorter durations more favorable. This technology is based on projections around lithium-ion (Li-ion), but it could also represent alternative battery chemistries that could achieve the cost and performance values assumed. We then consider two storage technologies representing longer duration technologies: LD1 and LD2. Of these two technology classes, LD1 is intended to capture technologies with somewhat lower power and energy costs but with lower round-trip efficiencies, potentially representing adiabatic CAES or pumped thermal storage. LD2 captures technologies with somewhat higher capacity and energy costs but also higher efficiencies, potentially representing PHS or longer duration batteries such as flow batteries. Finally, we include seasonal storage (SS), which has higher power-related costs, very low energy-related costs, and low round-trip efficiencies. This approximates a power-to-gas (e.g., hydrogen) or similar type of technology. Additionally, the charge power and discharge power for LD1 and seasonal storage can be independently optimized. The simultaneous assessment of different energy mix targets and multiple storage technologies, e.g., short-duration, long-duration, and seasonal storage, allows for a better understanding of the transition of storage requirements, e.g., from short-duration to long-duration and from long-duration to seasonal, as well as the operational policy for storage technologies as function of the energy mix target. Although we suggest representative technologies for each class, the techno-economic assumptions presented in Supplementary Table 1 are not intended to represent any specific energy storage installation. There is significant uncertainty regarding the technology evolution of storage, and some technologies might have very site-specific requirements, such as geological conditions for PHS and CAES[34]. Additional details regarding the input data are provided in Methods.

Table 1. ISO data and techno-economic assumptions for VRE, energy storage, and balancing technologies.

System property or parameter	ISO[32, §]						
	CAISO	ERCOT	ISONE	MISO	NYISO	PJM	SPP
2019 peak load (GW)	44.1	74.7	24.0	120.5	30.4	151.6	50.7
2019 total load (TWh)	219.5	383.8	118.3	667.9	155.8	787.3	270.4
2050 peak load (GW)	54.2	101.0	28.1	148.9	34.4	184.0	65.2
2050 total load (TWh)	269.2	519.1	138.8	825.5	176.1	955.8	348.3
Nuclear generation (% of 2019 total load)	7.4	10.8	25.2	15.4	28.7	35.5	6.0
Hydro generation (% of 2019 total load)	12.0	0.2	6.8	1.7	18.8	2.1	5.6
Other renewable generation (% of 2019 total load)	7.2	0.1	4.9	1.1	1.4	0.7	0.1

§ CAISO: California Independent System Operator (http://oasismap.caiso.com/mrioasis/logon.do); ERCOT: Electric Reliability Council of Texas (http://www.ercot.com/gridinfo); ISONE: Independent System Operator–New England (https://www.iso-ne.com/markets-operations/iso-express); MISO: Midcontinent Independent System Operator

(https://docs.misoenergy.org/marketreports/YYYYMMDD_rf_al.xls); NYISO: New York Independent System Operator (load data: http://mis.nyiso.com/public/P-58Blist.htm, generation data: http://mis.nyiso.com/public/P-63list.htm); PJM: Pennsylvania-Jersey-Maryland Power Pool (https://dataminer2.pjm.com/list); SPP: Southwest Power Pool (https://marketplace.spp.org/pages/generation-mix-historical).

VRE deployment and optimal energy storage portfolio

We use SDOM to analyze the effects of the energy mix on the optimal (least-cost) storage portfolio and operation as well as the optimal VRE deployment and curtailment. We provide results in this section primarily from CAISO and MISO because these tend to produce bookend results, with CAISO being dominated by solar PV deployments and MISO by wind. Full results are provided in the Supplementary Information. The optimal VRE mix for the other five ISOs is between that of these two systems. For CAISO, depending on the renewable energy mix targets, the optimal solar PV energy share varies from 42.0%–56.7%, and the optimal wind energy share varies from 17.8%–29.3% (Figure 1a). For MISO, these ranges are 9.5%–25.3% and 63.3%–72.7% for solar PV and wind, respectively (Figure 1b). Although the optimal mix of solar PV and wind power generation depends on a variety of factors, including electricity demand patterns, the differences in the optimal mix of solar PV and wind power generation between CAISO and MISO seem to be driven more by the differences in the resource quality between the two regions. For instance, the average capacity factor of the potential solar PV plants considered in this study is 22.3% and 21.3% for CAISO and MISO, respectively (Supplementary Figs. 9a and 12a). In contrast, the average capacity factor of the potential wind facilities is 24.1% and 48.3% for CAISO and MISO, respectively (Supplementary Figs. 9a and 12a). Using the proposed framework and assumptions, achieving a 100% renewable energy mix in CAISO would require deploying 96.5 GW of solar PV and 36.2 GW of wind power generation capacity. In contrast, achieving a 100% renewable energy mix in MISO would require deploying 146.8 GW of solar PV and 170.0 GW of wind power generation capacity. The results for the carbon-free energy mix targets are similar and are summarized in Supplementary Fig. 16. Regardless of the ISO and for energy share targets less than 95%, the optimal VRE curtailment monotonically increases with the share of carbon-free or renewable energy sources; however, the optimal VRE curtailment decreases significantly when moving from the 95% to the 100% energy share target. This results from the seasonal storage needed to achieve 100% renewable energy. At the lower values, it is more cost-effective to curtail renewable energy than to deploy expensive seasonal storage. The optimal VRE mix and curtailment for the other ISOs are summarized in Supplementary Figs. 17–21.

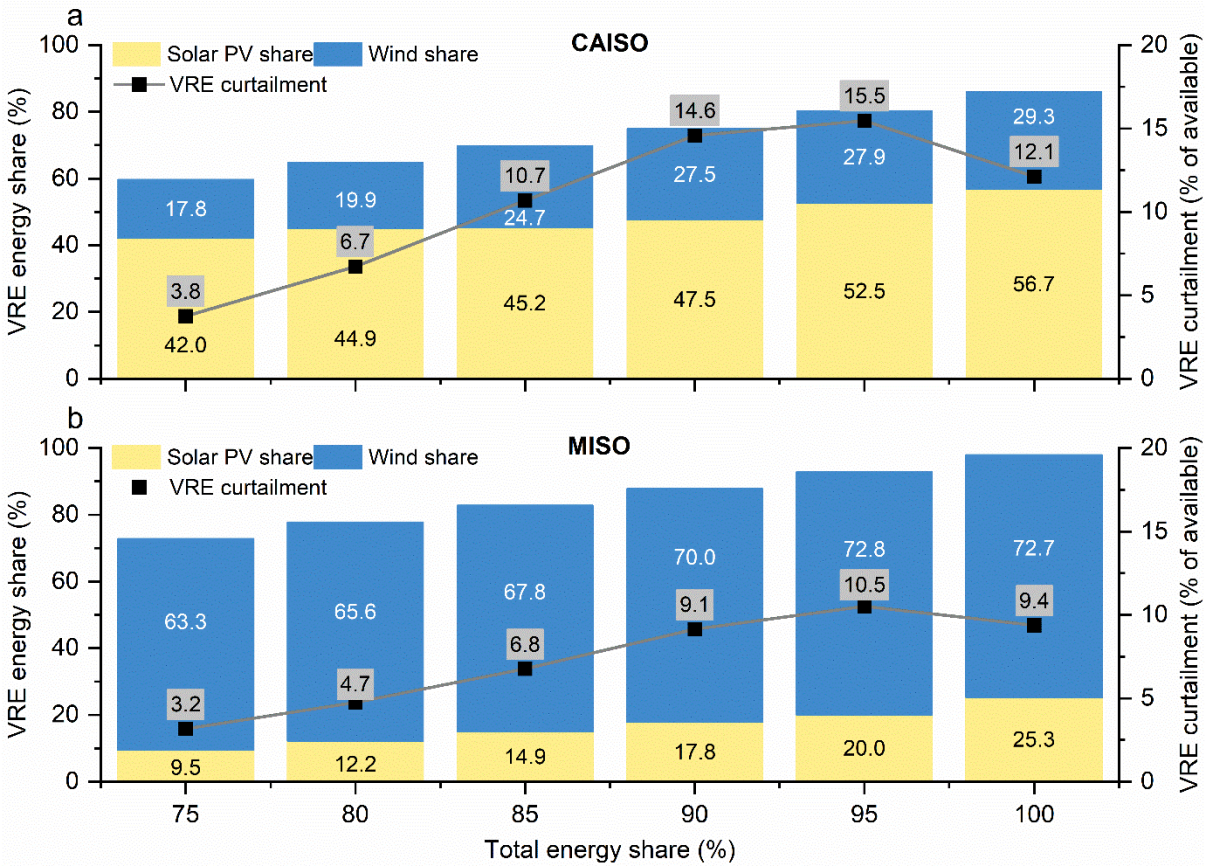

Figure 1. Optimal VRE mix and curtailment for renewable energy mix targets in CAISO (top) and MISO (bottom) in 2050. **a**, optimal VRE mix and curtailment for CAISO. **b**, optimal VRE mix and curtailment for MISO. The definitions of VRE share and curtailment are presented in Methods.

The optimal energy storage portfolios for the renewable energy mix targets for CAISO and MISO are summarized in Figure 2. The results for the other energy mix targets and ISOs are summarized in Supplementary Figs. 22–27. The results follow previously demonstrated trends, including increased storage capacity as a function of VRE deployment and a transition to longer-duration storage. In general, the required total storage power capacity increases monotonically with the renewable or carbon-free energy mix depending on the power system. Seasonal storage is not deployed before a renewable mix of approximately 85%–90%. We also see significant variation in the amount of seasonal storage deployed based on the energy mix. For these energy mix targets, the required proportion of seasonal storage power capacity is less for CAISO (e.g., ~24% of total storage power capacity) than for the other ISOs (e.g., 35%–54% of total storage power capacity). In contrast, the required discharge duration is greater for CAISO for both short-duration (SD) and seasonal (SS) storage technologies. For instance, for CAISO the required discharge duration ranges from 2.1 hours–5.1 hours for short-duration and from 44 days–59 days (~1.5 to ~2 months) for seasonal storage technology. For MISO, the required discharge duration ranges from 1.4 hours–2.0 hours for short-duration and from 5.6 days–14.3 days for seasonal storage

technology (the results for carbon-free energy mix targets are similar). This difference between solar PV-driven systems (e.g., CAISO) and wind-driven systems (e.g., MISO) is driven by the combination of both diurnal and seasonal coincidence with load and the inherently higher spatial variability of wind, particularly in the diurnal timeframe. This result follows previous analysis that demonstrates the impact of the spatial variability of wind[27]. Achieving the lowest cost for a 100% renewable energy mix, however, would require significant deployment of seasonal energy storage.

In addition, we see significant potential benefits for technologies that can decouple charging/discharging power capacities. We allow this for LD1 and the seasonal storage technologies (see Methods). Figure 3. shows that the LD1 charging/discharging capacity ratio for CAISO increases monotonically and is greater than 1 for 80% or greater energy mix targets. This results from the relatively short periods of surplus energy available during the day (requiring higher charging power), followed by long periods of somewhat lower load overnight, which requires less discharging power. In contrast, regardless of the energy target, the LD1 power capacity ratio is less than 1 for the other ISOs (wind-driven power systems). The seasonal storage power capacity ratio tends to decrease with the renewable energy target and is less than 1 for the 100% carbon-free or renewable energy mix regardless of the ISO; thus, along with duration, the charging-to-discharging power ratio is an important parameter and depends on the selected region and system conditions. To provide insight into how techno-economic assumptions could impact the optimal VRE mix and storage portfolio, we implement a sensitivity analysis for the 100% carbon-free and 100% renewable energy mix targets in CAISO and MISO (see Supplementary Section 8). The results are summarized in Supplementary Figs. 32–35.

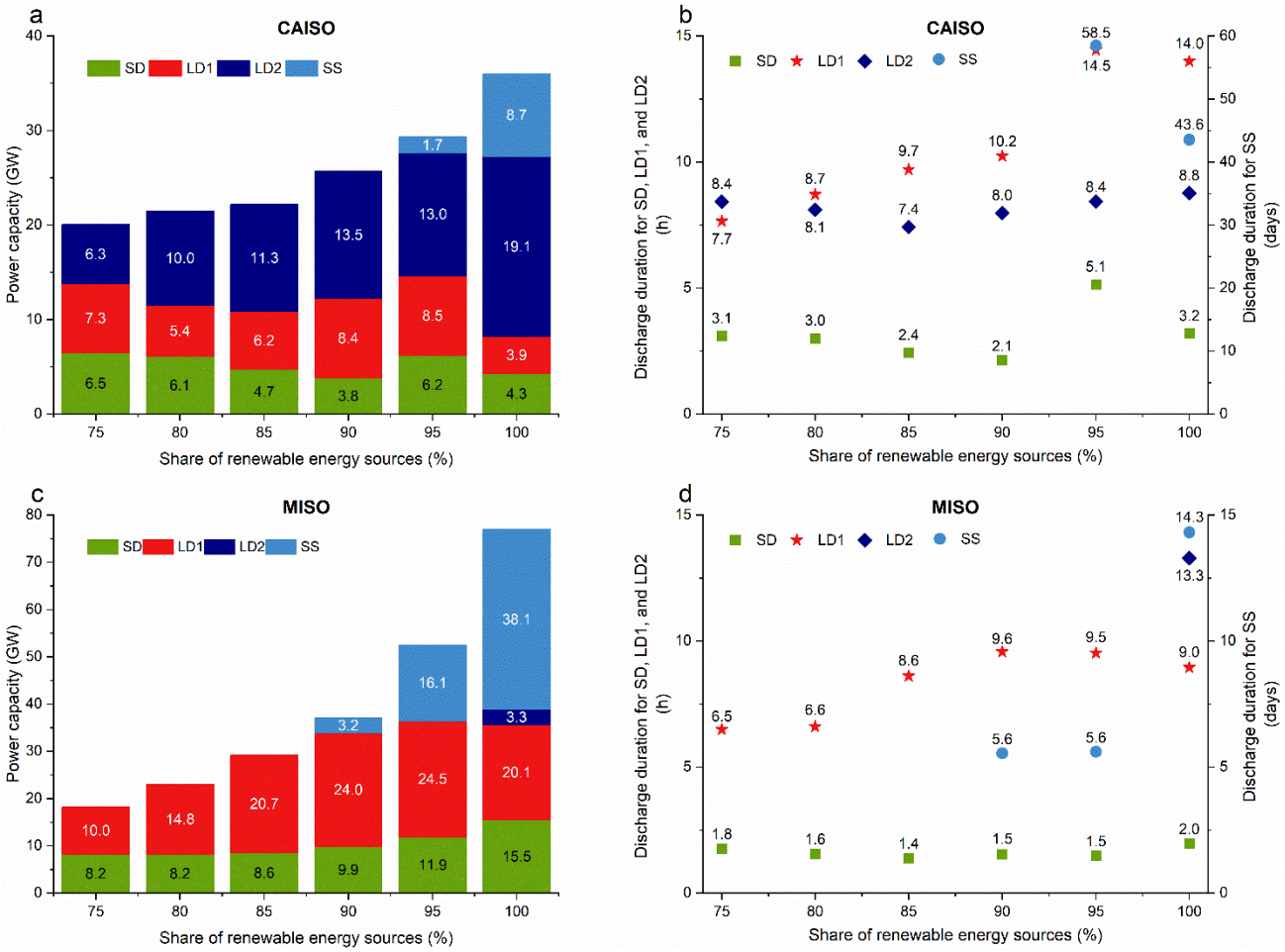

Figure 2. Optimal storage portfolio for renewable energy mix targets in CAISO (top) and MISO (bottom) in 2050. Storage power capacity by type is shown in the left plots (Fig. 2.**a** for CAISO and Fig. 2.**c** for MISO). Storage discharge durations by technology type are shown in the right plots (Fig. 2.**b** for CAISO and Fig. 2.**d** for MISO). The average power capacity is reported for storage technologies that can decouple charging/discharging power capacity (LD1 and SS; see Methods). The definition of storage discharge duration is presented in Methods.

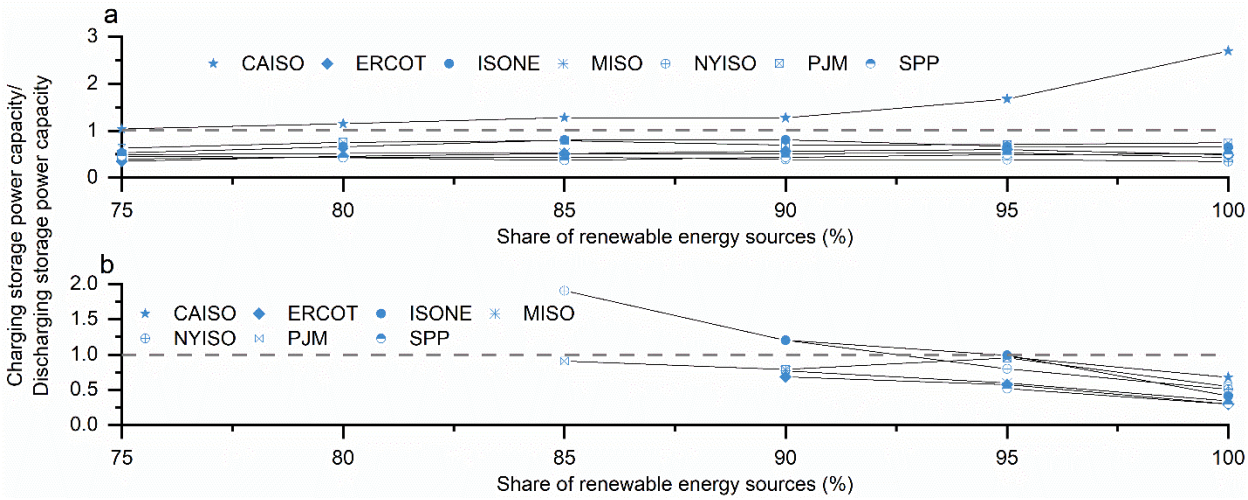

Figure 3. Optimal charging/discharging power capacity ratio for storage technology. **a**. optimal charging/discharging power capacity ratio for the LD1 and renewable energy mix targets. **b**. optimal charging/discharging power capacity ratio for the seasonal storage and renewable energy mix targets. Results for the carbon-free energy mix targets are shown in Supplementary Fig. 28.

To better understand how power and energy capacity storage requirements vary as a function of VRE deployment, we use normalized metrics based on the average residual load (see Methods); see Figure 4. Note that this analysis is based on the seven ISOs and the six carbon-free or renewable energy mix targets (84 scenarios). First, the normalized total storage power capacity is expressed as a function of the normalized VRE installed generation capacity (Figure 4a). The normalized total storage power capacity increases linearly (Pearson correlation coefficient = 0.95) with the normalized VRE capacity. In contrast, depending on the ISO, the normalized total storage energy capacity increases exponentially with the corresponding energy share (Figure 4b). These findings are consistent with previous work[27].

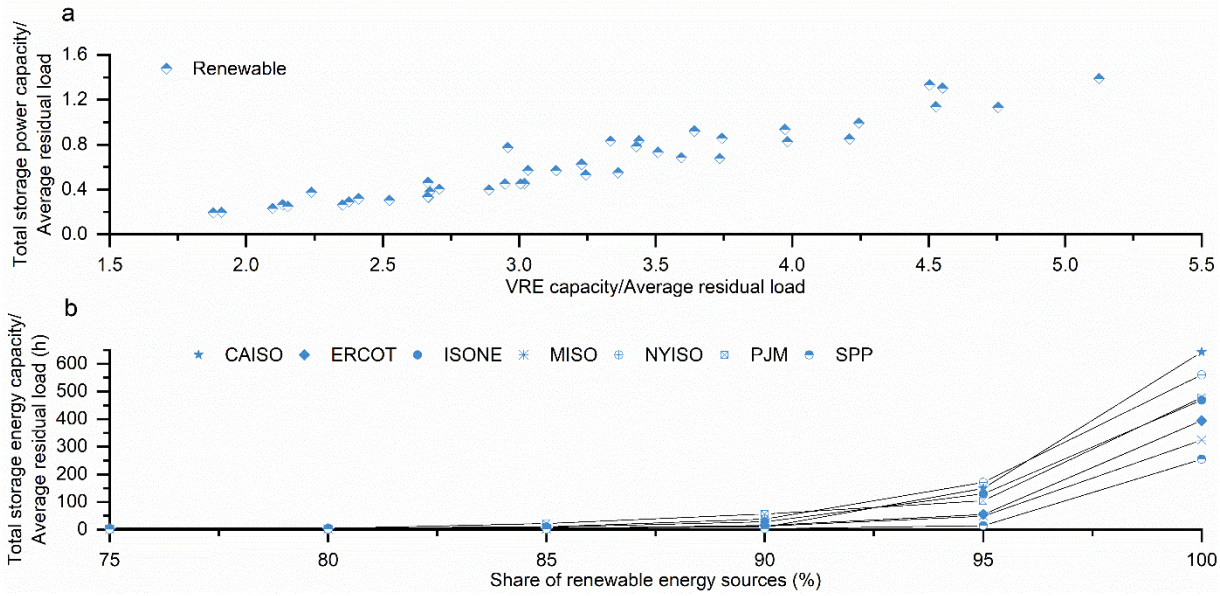

Figure 4. Total storage power and energy capacity for renewable scenarios as a function of VRE deployment in 2050. **a**, normalized total storage power capacity as a function of the normalized VRE capacity across all the ISOs. **b**, normalized total energy storage capacity as a function of the renewable energy share. Results for the carbon-free energy mix targets are shown in Supplementary Fig. 29.

Operation of energy storage across different timescales

Improving the understanding of the operational behavior of the storage portfolio can support the research community and industry by: (i) demonstrating the potential role for each technology to support grid operations, (ii) providing technology companies an understanding of the operational expectations for different types of storage, and (iii) providing information regarding expected operation for others that want to model this technology but will not perform a detailed operational analysis.

The state of charge (SOC) for each storage technology and 100% renewable energy mix in CAISO and MISO are shown in Figure 5. In CAISO (Figure 5a), short duration, LD1, and LD2 generally discharge storage between 16:00–20:00 and charge storage between 08:00–16:00. This accommodates the solar profile, the dominant renewable generation technology in CAISO. The seasonal storage SOC profile exhibits strong seasonal behavior, charging in the spring and summer and discharging in the fall and winter. These findings are similar for MISO (Figure 5b), except that LD1 and LD2 exhibit more multiday energy shifting than daily arbitrage.

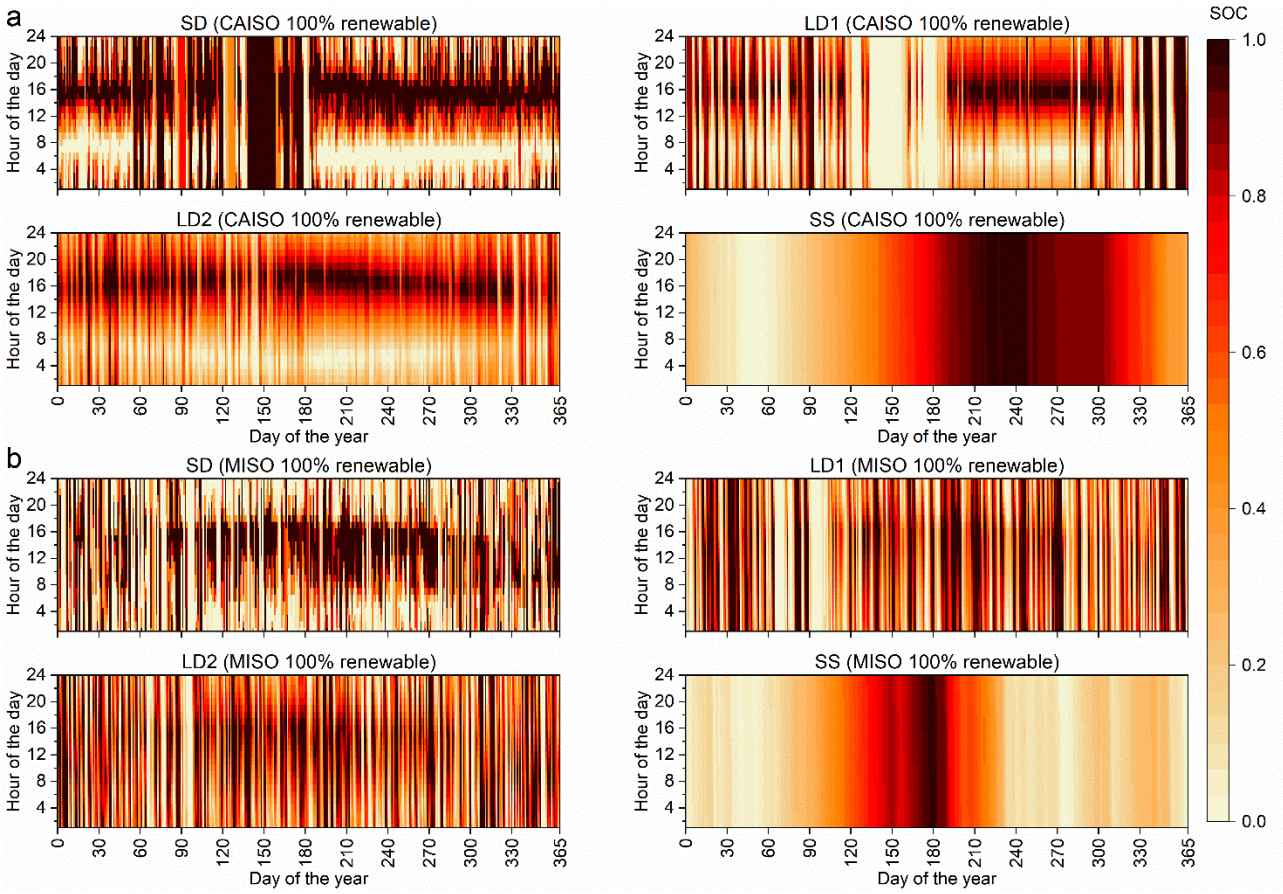

Figure 5. Normalized state of charge (SOC) for storage devices in CAISO and MISO. **a,** normalized SOC for storage devices for CAISO 100% renewable energy mix. **b,** normalized SOC for storage devices for MISO 100% renewable energy mix. The definition of normalized SOC is presented in Methods. SOC=1 (dark red) implies that the storage device is full. SOC=0 (light red) implies that the storage device is empty. The normalized SOC for storage devices in the CAISO and MISO 100% carbon-free energy mix are presented in Supplementary Fig. 31.

The equivalent annual discharging cycles for each technology create a comparable measure of cycling between regions and technologies and more clearly show the extent to which they are operated, as shown in Figure 6a. Equivalent annual discharging cycles are defined as the sum of all partial discharging cycles throughout the year (see Methods). There is a significant difference between the solar PV-dominated CAISO system and wind-dominated systems. All short- and long-duration technologies cycle more often in CAISO to accommodate the diurnal cycling of solar PV, whereas those technologies cycle less often in the other ISOs. Seasonal storage devices have significantly lower equivalent cycles than other technologies mostly because of the large size of the energy storage capacity and relatively low round-trip efficiency.

As the carbon-free or renewable share approaches 100%, one storage device is sometimes used to charge another storage device, i.e., storage-to-storage operation. The

resulting fraction of annual storage charging energy that is used to charge other storage devices is between 6%–12% of all charging energy for the 100% renewable energy mix target (Figure 6b) and occurs across all ISOs. The behavior begins near the 90% target for carbon-free scenarios and the 85% target for renewable scenarios. Examining the average time of day (Figure 6c) shows that in CAISO this behavior occurs mostly in the evening, and on limited occasions seasonal storage device is used to charge other storage technologies. The overall behavior is consistent with excess generation patterns for solar. In CAISO (Figure 6d), this is related to periods of excess generation in the spring and summer associated with low load and high renewable production. Although multiple storage processes increase the overall energy losses, these losses are offset by the increased utilization of the resources and reduce the overall storage capacity needs of the system. As a result, transferring energy between storage devices effectively increases the amount of energy that can be stored in the seasonal storage device.

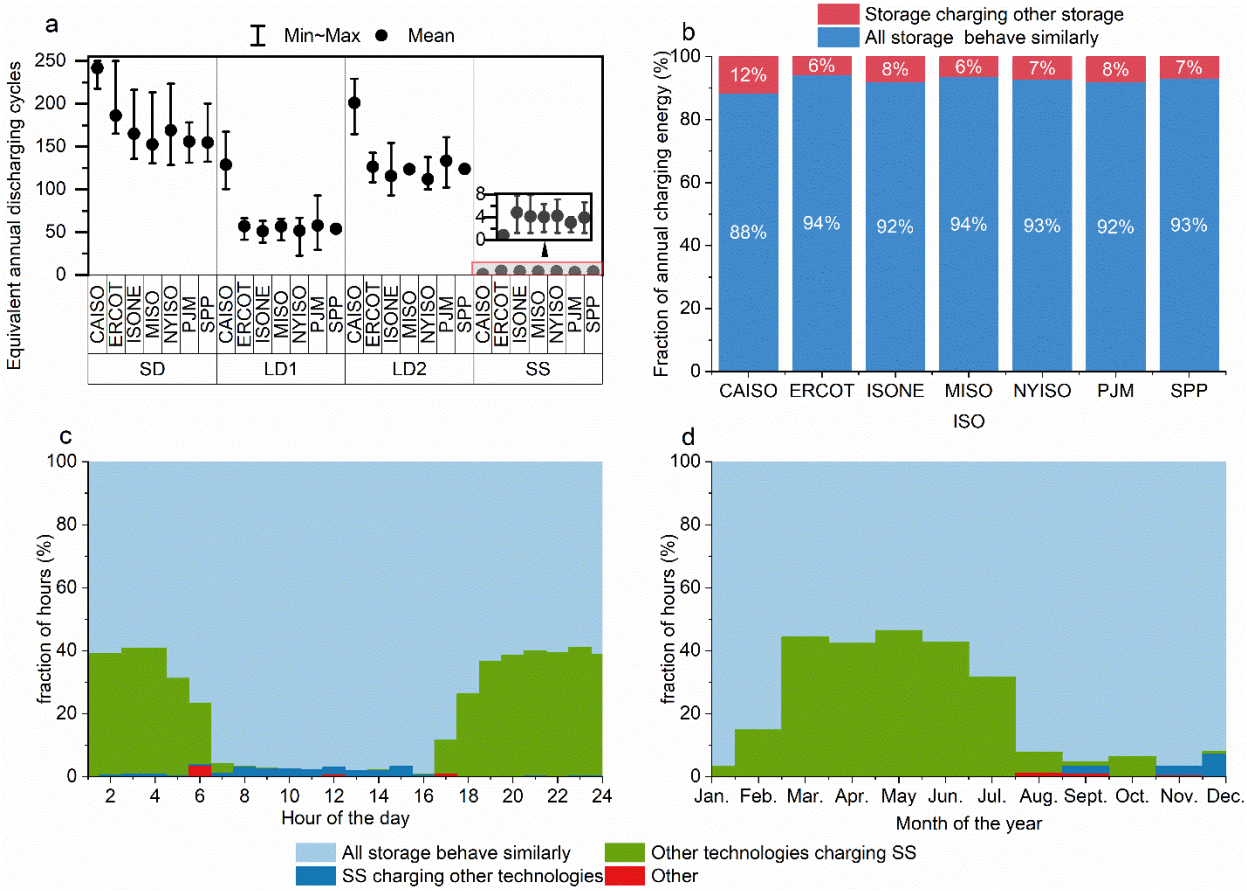

Figure 6. Metrics for storage operation. **a**, equivalent annual discharging cycles for each storage technology and each ISO across all carbon-free and renewable energy mix targets: 75%, 80%, 85%, 90%, 95%, and 100%. **b**, breakdown of storage energy used to charge other storage for each ISO with a 100% renewable energy mix target. **c**, hourly average breakdown of storage that charges other storage for CAISO with a 100% renewable energy mix target. **d**, monthly average breakdown of storage that charges other storage for CAISO

with a 100% renewable energy mix target. “Other” includes LD1 charging short duration, LD2 charging short duration, etc.

Energy cost and cost of avoided CO_2 emissions

This analysis follows previous work that demonstrates a substantial increase in costs as a system approaches 100% renewable energy mix[31,35]. Figure 7 provides an example of the average energy cost (US$ per MWh) and the cost of avoided carbon dioxide (CO_2) emissions (US$ tonne^{-1}) across the various regions analyzed (see Methods). In SPP, the ISO with the lowest average energy costs, a high renewable energy mix can be achieved at electricity costs ranging from US$38.1 MWh^{-1} to US$48.2 MWh^{-1} for renewable energy mix, depending on the energy mix target. In contrast, energy costs for CAISO vary from US$51.6 MWh^{-1} to US$80.0 MWh^{-1} for renewable energy mix, depending on the target. Results are similar for carbon-free energy mix scenarios. Note that the capacity factor for the gas combined-cycle balancing unit varies from 8.4%–39.6%, depending on the ISO and the energy mix target. Based on this range for the capacity factor, the estimated levelized cost of energy for a gas combined-cycle unit with carbon capture and sequestration varies from US$77.8 MWh^{-1} (CAISO 75% carbon-free energy mix, 39.6% capacity factor for gas combined cycle) to US$229.6 MWh^{-1} (ISONE 95% renewable energy mix, 8.4% capacity factor for gas combined cycle) [36]. It is noteworthy that this study did not consider the monetization of VRE externalities, e.g., climate and air-quality benefits, which could reduce the costs of carbon-free or renewable power systems. As a reference, in 2015, the estimated combined climate and air-quality marginal benefit was approximately 2020 US$79.7 MWh^{-1} and 2020 US$43.7 MWh^{-1} for wind and solar PV power in the United States, respectively[37]. Regarding the cost of avoided CO_2 emissions, an 85% carbon-free or renewable energy mix can be achieved at a cost of US$66.0 per tonne or less regardless of the ISO. Excluding CAISO, a 90% carbon-free or renewable energy mix can be achieved at a cost of US$63.5 per tonne or less in all other ISOs. In general, the cost of avoided carbon emissions is higher in CAISO (a PV-driven system) than in the other ISOs.

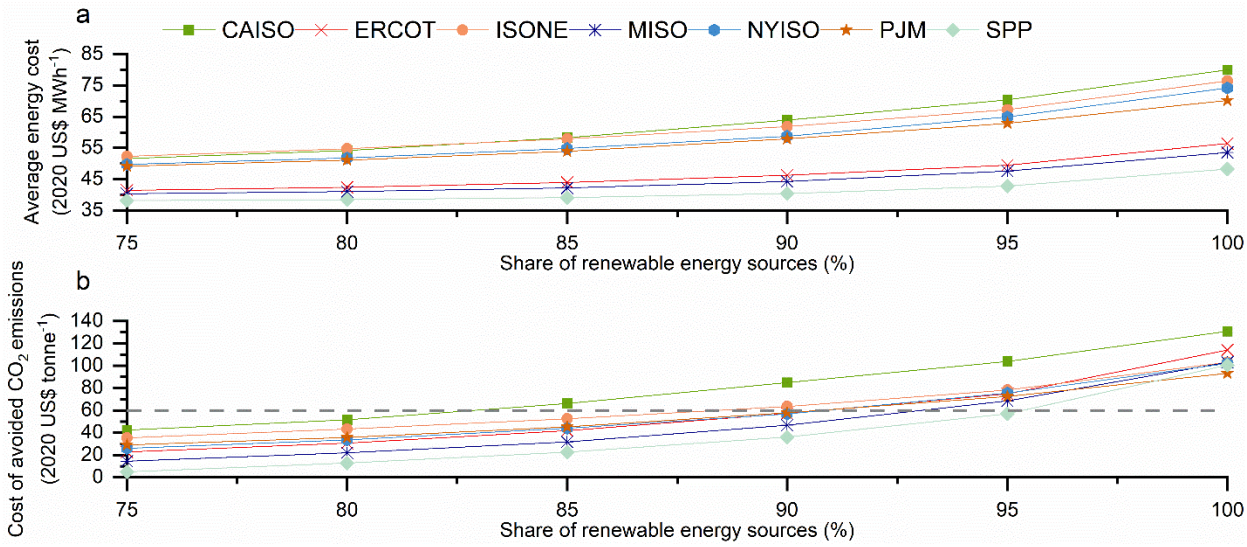

Figure 7. Energy cost and cost of avoided CO_2 emissions. **a**, energy cost for renewable energy mix targets. **b**, cost of avoided CO_2 emissions for renewable energy mix targets. Gray dashed line in Fig. 7b represents a cost of US$60.0 per tonne for avoided CO_2 emissions. Results for the carbon-free scenarios are summarized in Supplementary Fig. 30. Additionally, the average energy cost and the cost of avoided CO_2 emissions for the sensitivity scenarios are summarized in Supplementary Fig. 35.

Conclusions

Energy storage could play a pivotal role in enabling high and ultrahigh carbon-free or renewable power systems, but there is a lack of understanding of the scale and operation of the optimal wind, solar photovoltaic power, and energy storage portfolio to achieve these energy mix targets. The effects of energy mix on the optimal energy storage portfolio and the conditions and scale of VRE deployment to transition from short-duration to long-duration and seasonal storage are not comprehensively considered in the literature. In this study, therefore, we developed and implemented a high-temporal and high-spatial resolution grid planning framework to provide detailed insight into the optimal power generation and storage portfolio, based on four generic storage technologies, for seven independent system operators across the United States.

Our results indicate that carbon-free and renewable energy targets of up to 80% are achieved with economic curtailment and a combination of short- and long-duration energy storage for the cost and performance assumptions used. There is a point between 80% and 95% where seasonal storage becomes cost-competitive, depending on the specific power system.

Achieving a 100% carbon-free or renewable energy target can benefit from a significant portion of the storage portfolio to come from seasonal storage (between 24% and 54% of the total power capacity). As the energy mix target approaches 100%, the operation of short- and long-duration storage devices to charge seasonal storage devices, i.e., storage-

to-storage operation, becomes cost-effective. This accounts for between 6% and 12% of the energy used to charge the storage devices for the 100% renewable energy mix in CAISO.

Considering all scenarios, short-duration energy storage provides predominantly diurnal energy shifting with between 1.4 and 5.1 hours of discharge capacity, high cycling with 129–250 equivalent annual discharge cycles, and accounts for between 8%–56% of the storage portfolio power capacity. With higher power capital expenditures than the short-duration storage technology but lower energy capacity cost and efficiency, long-duration storage technologies provide diurnal energy shifting and also some inter-day shifting with durations between 4.9–16.1 hours at discharge power, depending on the technology. Cycling behavior is driven by the round-trip efficiency, i.e., technologies with a higher efficiency tend to have higher number of equivalent cycles. Long-duration storage technologies perform between 23 and 161 equivalent annual discharge cycles for all ISOs except CAISO, which has 100–229 equivalent discharge cycles. This is equivalent to a discharge capacity factor of 2.4%–29%. Long-duration storage technologies comprised between 28%–87% of the total storage portfolio power capacity across all scenarios. Last, although seasonal storage is assumed to have a higher power capacity cost and a lower round-trip efficiency than any other technology, the energy capacity cost assumption for seasonal storage is more than an order of magnitude lower than the nearest competitors, i.e., long-duration storage technologies. As a result, seasonal storage takes the role of inter-day and intra-season storage with discharge durations between 3.6–58.5 days. Because of the large storage level and low round-trip efficiency, equivalent annual discharge cycles are between 0.8–7.9 for seasonal storage, equal to a discharge capacity factor of 7.7%–27%. Seasonal storage is not installed in every system or for every energy target, but when installed, it comprises between 2%–54% of the storage portfolio power capacity and is particularly important for achieving 100% energy targets. Regardless of the power system and for energy share targets below 95%, the optimal solar photovoltaic and wind power curtailment monotonically increases with the share of carbon-free or renewable energy sources. Driven by the deployment of seasonal storage capacity, curtailment decreases significantly when moving from the 95% to the 100% energy mix target. Thus, despite the large-scale deployment of different storage technologies, power curtailment is a cost-effective flexibility option for the integration of variable renewable energy sources.

Additionally, using the average residual load as a normalization factor, it was observed that the normalized total storage power capacity increases linearly with the normalized VRE capacity, whereas normalized total storage energy capacity increases exponentially with the corresponding energy share. Finally, this study shows that a high carbon-free or renewable energy mix can be achieved at electricity costs (including capital and operational expenditures) ranging from US$38.1 MWh^{-1} to US$80.4 MWh^{-1}, which is likely less than the cost of operating with gas combined- cycle plus carbon capture-and-sequestration units, e.g., US$77.8 MWh^{-1}–US$229.6 MWh^{-1}. Moreover, it was estimated that an 85% carbon-free or renewable energy mix can be achieved at a cost of avoided CO_2 emissions of US$66.0 per tonne or less, regardless of the power system.

Methods

SDOM mathematical formulation

The high-temporal- and high-spatial-resolution grid planning framework SDOM is formulated as a mixed-integer linear programming (MILP) model. SDOM optimizes both capacity expansion for select resources (VRE, gas combined cycle, and storage technologies) as well as storage operations. SDOM minimizes the total power system capital and operational cost for a given carbon-free or renewable energy target—e.g., an 80% renewable energy share—for a 1-year operation window assuming no transmission constraints, e.g., copperplate approach and perfect foresight of electricity demand and VRE generation. Note that a multiyear analysis could be more appropriate. For instance, simulation-based multiyear analyses allow for the assessment of the impacts of interannual variability of VRE generation and load on storage requirements[31,38]; however, multiyear chronological optimization analyses with hourly resolution are computationally challenging—based on current computing capabilities—and therefore it is left for future work.

We use index h to denote hours in the analysis period, e.g., 8,760 hours represented by the set H ($h \in H$). For instance, $H = \{1,2,3,\ldots,8760\}$. Additionally, SDOM considers a set (J) of storage technologies (indexed by j, i.e., $j \in J$), a set (K) of potential solar PV plants (indexed by k, i.e., $k \in K$), and a set (W) of potential wind plants (indexed by w, i.e., $w \in W$).

The objective function is to minimize the total annual system cost (TSC), as defined in equation 1. The total system cost includes the following cost components for VRE plants: capital cost ($SolarCapex_k$ for solar PV and $WindCapex_w$ for wind), transmission investment cost ($SolarTcost_k$ for solar PV and $WindTcost_k$ for wind), and FO&M cost ($SolarFOM_k$ for solar PV and $WindFOM_k$ for wind). The annualization of the VRE investment costs is represented by corresponding capital recovery factor: parameters $CRFs$ and $CRFw$ for solar PV and wind power plants, respectively. Each potential VRE plant has a maximum power capacity to be installed (determined by the reV model[33]): $CapSolar_k$ for solar PV and $CapWind_w$ for wind. Then, a positive continuous variable is used to select a given fraction (from 0 to 1) of that maximum power capacity of the plant: variable $YSolar_k$ for solar PV and variable $YWind_w$ for wind.

Additionally, the objective function considers the following cost components for storage technologies: power capacity capital cost ($PSCapex_j$), energy capacity capital cost ($ESCapex_j$), FO&M cost (FOM_j), and VO&M cost (VOM_j). Note that some storage technologies—e.g., CAES (generic technology LD1) and hydrogen (generic technology SS)—allow for decoupling charging and discharging power capacity; thus, SDOM uses a positive continuous variable for the installed charging power capacity ($CapPC_j$) and a different positive continuous variable for the installed discharging power capacity ($CapPD_j$). Accordingly, the parameter CR_j is used to denote the ratio of the cost for charging power capacity to the total power-related cost. Note that $CR_j = 0.5$ for technologies that do not allow for decoupling charging and discharging power capacity—Li-ion batteries (generic technology SD) and PHS (generic technology LD2). Capital cost for storage technologies is

annualized based on the corresponding capital recovery factor ($CRFst_j$). Regarding energy capacity, SDOM also optimizes the energy storage capacity ($CapES_j$) for each technology. Total VO&M cost is expressed as a function of the hourly discharging power for each storage technology ($PD_{h,j}$).

Finally, the following cost components for the balancing unit—i.e., gas combined cycle—are included in the total system cost: capital cost ($BUCapex$), fuel cost, FO&M cost, ($FOMbu$), and VO&M cost ($VOMbu$). Total fuel cost is calculated based on the fuel price ($FuelPrice$), the heat rate ($HRbu$), and the hourly power generation from the balancing unit ($GenBU_h$). The investment cost associated with the balancing unit is annualized using the corresponding capital recovery factor ($CRFbu$). Additionally, capital and FO&M costs are calculated based on the installed power capacity of the balancing unit ($CapBU$).

$$
\begin{aligned}
Min\ TSC = \sum_{k \in K} (& CRFs \cdot (SolarCapex_k + SolarTcost_k) + SolarFOM_k \\
& \cdot CapSolar_k \cdot YSolar_k \\
& + \sum_{w \in W} (CRFw \cdot (WindCapex_w + WindTcost_k) + WindFOM_k) \\
& \cdot CapWind_w \cdot YWind_w \\
& + \sum_{j \in J} CRFst_j \\
& \cdot \big(CR_j . PSCapex_j \cdot CapPC_j + (1 - CR_j) \cdot PSCapex_j \cdot CapPD_j \\
& + ESCapex_j \cdot CapES_j\big) + \sum_{j \in J} CR_j \cdot FOM_j \cdot CapPC_j \\
& + \sum_{j \in J} (1 - CR_j) \cdot FOM_j \cdot CapPD_j + \sum_{j \in J} VOM_j \cdot \sum_{h \in H} PD_{h,j} + (CRFbu \\
& \cdot BUCapex + FOMbu) \cdot CapBU + (FuelPrice \cdot HRbu + VOMbu) \\
& \cdot \sum_{h \in H} GenBU_h
\end{aligned}
\qquad 1
$$

The capital recovery factor for solar PV, wind, energy storage, and the balancing unit is calculated using equations 2, 3, 4, and 5, respectively. The discount rate is represented by scalar r (6.0%). Scalars τs and τw denote the lifetime (in years) for solar PV (30 years[36]) and wind power plants (30 years[36]), respectively. Additionally, parameter τ_j denotes the lifetime for the storage technology j. Finally, scalar τbu represents the lifetime for the balancing unit (gas CC) (30 years)[36].

$$
CRFs = \frac{r \cdot (1 + r)^{\tau s}}{(1 + r)^{\tau s} - 1} \qquad 2
$$

$$CRFw = \frac{r \cdot (1+r)^{\tau w}}{(1+r)^{\tau w} - 1} \quad (3)$$

$$CRFst_j = \frac{r \cdot (1+r)^{\tau_j}}{(1+r)^{\tau_j} - 1} \quad \forall\, j \in J \quad (4)$$

$$CRFbu = \frac{r \cdot (1+r)^{\tau bu}}{(1+r)^{\tau bu} - 1} \quad (5)$$

The power balance constraint for the system is expressed in equation 6. Parameter $Load_h$ represents the total hourly load of the power system. Positive continuous variable $PC_{j,h}$ denotes the hourly charging power for the storage technologies. Additionally, parameters $Nuclear_h$, $Hydro_h$, and $OtherRen_h$ denote the time series for the power generation from the existing nuclear, hydro, and other renewable (e.g., biomass and geothermal) power plants, respectively. Scalar $\alpha_{nuclear}$ is used to activate nuclear generation for the carbon-free energy targets ($\alpha_{nuclear} = 1$) or to deactivate nuclear generation for the renewable energy targets ($\alpha_{nuclear} = 0$). Similarly, positive continuous variables $GenSolar_h$ and $GenWind_h$ represent hourly power generation (used by the grid) from new solar PV and wind power plants, respectively.

$$Load_h + \sum_{j \in J} PC_{j,h} - \alpha_{nuclear} \cdot Nuclear_h - Hydro_h - OtherRen_h - GenSolar_h - GenWind_h - \sum_{j \in J} PD_{j,h} - GenBU_h = 0 \quad \forall\, h \in H \quad (6)$$

The carbon-free or renewable energy mix target ($GenMixTarget$) is enforced by equality constraint 7, which includes energy losses associated with the operation of storage technologies. Additionally, the power generation constraint for solar PV and wind facilities is described in equations 8 and 9, respectively. Hourly solar PV and wind curtailment is represented by positive continuous variables $CurtSolar_h$ and $CurtWind_h$, respectively. Moreover, the hourly capacity factor for solar PV and wind facilities is represented by parameters $CFSolar_{k,h}$ and $CFWind_{w,h}$, respectively. The required power capacity for the gas combined-cycle balancing unit is defined by equation 10.

$$\sum_{h \in H} GenBU_h = (1 - GenMixTarget) \cdot \sum_{h \in H} \left(Load_h + \sum_{j \in J} \left(PC_{j,h} - PD_{j,h} \right) \right) \quad (7)$$

$$GenSolar_h + CurtSolar_h = \sum_{k \in K} CFSolar_{k,h} \cdot CapSolar_k \cdot YSolar_k \quad \forall\, h \in H \tag{8}$$

$$GenWind_h + CurtWind_h = \sum_{w \in W} CFWind_{w,h} \cdot CapWind_w \cdot YWind_w \quad \forall\, h \in H \tag{9}$$

$$GenBU_h \leq CapBU \quad \forall\, h \in H \tag{10}$$

The installed charging and discharging power capacity for storage technologies is constrained by the maximum power capacity ($PSmax_j$), as defined by equations 11 and 12, respectively; however, these power capacities should be the same for storage technologies that do not allow for decoupling charging and discharging power capacity, as described by equation 13. This subset of technologies is defined by set $ND = \{Li - Ion\ (SD), PHS\ (LD2)\}$. The maximum power capacity could be defined based on the peak load of the system. Similarly, the installed energy capacity for each storage technology is constrained by the minimum ($DSmin_j$) and maximum ($DSmax_j$) discharge duration, as defined by equations 14 and 15, respectively. The minimum discharge duration is defined based on the temporal resolution used by SDOM, i.e., 1 hour, whereas the maximum discharge duration could be defined based on technical specifications (or industrial practices)—e.g., 12 hours for Li-ion batteries (generic technology short duration) or the estimated potential for a specific technology and power system territory, particularly for CAES, PHS, and hydrogen storage[39–41]. Note that we make the following assumptions regarding the efficiency of the storage technologies: (i) the self-discharge rate is negligible, and (ii) the efficiencies for charging and discharging are equal; thus, $n_j^{charging} = n_j^{discharging} = \sqrt{n_j}$, where parameter η_j represents the round-trip efficiency for the storage technology j. Additionally, hourly charging and discharging power should be less than the corresponding power capacity, as expressed by equations 16 and 17. Regarding the operation of storage technologies, SDOM considers that storage devices cannot charge and discharge simultaneously, as expressed by equations 18 and 19. Binary variable $YS_{j,h}$ is used to define the operation mode of the storage devices—i.e., $YS_{j,h}$=1 for charging, and $YS_{j,h}$=0 for discharging. Note that for market-based operation of storage devices, the simultaneous charging and discharging could be beneficial during time periods with negative prices[25]. The energy balance for the SOC of storage units ($SOC_{j,h}$) is represented by equation 20, whereas equation 21 is used to endogenously optimize the initial SOC of storage units. Using equation 21 to appropriately set the initial SOC is particularly important for seasonal storage devices. The SOC of storage should be less than the energy capacity of the storage devices, as expressed by equation 22. Finally, to limit the degradation of the short-duration storage technology (SD), e.g., Li-ion batteries, constraint 23 is included to limit the equivalent number of cycles per year based on the cycle life ($MaxCycles_{SD}$), e.g., 3250[22], and the corresponding lifetime (τ_{SD}). The domain for each variable used in the mathematical formulation of SDOM is defined in equations 24–29. Note

that SDOM neglects ramp rates, reserve requirements, and subhourly VRE fluctuations; however, it is likely that these items could be addressed by the diversity, rapid response, and installed capacity of the storage technologies considered in this study. For instance, regarding the flexibility, e.g., the ability of the power system to respond to variability and uncertainty in load and power generation (primarily addressing high net load ramp rates), the maximum net load up ramps for 100% renewable energy mix target are 34.0 GW/h and 48.1 GW/h for CAISO and MISO, respectively (please see Supplementary Fig. 36). Additionally, the maximum net load down ramps for 100% renewable energy mix target are 31.4 GW/h and 43.2 GW/h for CAISO and MISO, respectively (please see Supplementary Fig. 36). On the other hand, the total optimal deployment of energy storage power capacity for 100% renewable energy mix target is 36.0 GW and 77.0 GW for CAISO and MISO, respectively. Note that the corresponding optimal discharge duration for the storage technologies is greater than 2 hours. Moreover, the response time for the storage technologies used as a reference in this study, e.g., Li-ion, CAES, PHS, and hydrogen, is in the order of minutes or seconds (very high ramp rates)[42]. SDOM is implemented in GAMS[43] as a MILP model and solved with CPLEX[44], and the relative optimality gap was set to 3%.

$$CapPC_j \leq PSmax_j \quad \forall\, j \in J \tag{11}$$

$$CapPD_j \leq PSmax_j \quad \forall\, j \in J \tag{12}$$

$$CapPC_j = CapPD_j \quad \forall\, j \in ND \tag{13}$$

$$CapES_j \geq DSmin_j \cdot \frac{CapPD_j}{\sqrt{\eta_j}} \quad \forall\, j \in J \tag{14}$$

$$CapES_j \leq DSmax_j \cdot \frac{CapPD_j}{\sqrt{\eta_j}} \quad \forall\, j \in J \tag{15}$$

$$PC_{j,h} \leq CapPC_j \quad \forall\, h \in H, j \in J \tag{16}$$

$$PD_{j,h} \leq CapPD_j \quad \forall\, h \in H, j \in J \tag{17}$$

$$PC_{j,h} \leq PSmax_j \cdot YS_{j,h} \quad \forall\, h \in H, j \in J \tag{18}$$

$$PD_{j,h} \leq PSmax_j \cdot (1 - YS_{j,h}) \quad \forall\, h \in H, j \in J \tag{19}$$

$$SOC_{j,h} = SOC_{j,h-1} + \sqrt{\eta_j} \cdot PC_{j,h} - \frac{PD_{j,h}}{\sqrt{\eta_j}} \quad \forall\, h \in H, h > 1, j \in J \tag{20}$$

$$SOC_{j,h=1} = SOC_{j,h=|H|} + \sqrt{\eta_j} \cdot PC_{j,h=1} - \frac{PD_{j,h=1}}{\sqrt{\eta_j}} \quad \forall\, j \in J \tag{21}$$

$$SOC_{j,h} \leq CapES_j \quad \forall\, h \in H, j \in J \tag{22}$$

$$\sum_{h \in H} PD_{SD,h} \leq \frac{MaxCycles_{SD}}{\tau_{SD}} \cdot CapES_{SD} \tag{23}$$

$$GenSolar_h \subseteq \mathbb{R}_{\geq 0}, CurtSolar_h \subseteq \mathbb{R}_{\geq 0}, GenWind_h \subseteq \mathbb{R}_{\geq 0}, \\ CurtWind_h \subseteq \mathbb{R}_{\geq 0}, GenBU_h \subseteq \mathbb{R}_{\geq 0} \quad \forall\, h \in H \tag{24}$$

$$YSolar_k \in [0,1] \subseteq \mathbb{R}_{\geq 0} \quad \forall\, k \in K \tag{25}$$

$$YWind_w \in [0,1] \subseteq \mathbb{R}_{\geq 0} \quad \forall\, w \in W \tag{26}$$

$$CapBU \subseteq \mathbb{R}_{\geq 0} \tag{27}$$

$$CapPC_j \subseteq \mathbb{R}_{\geq 0}, CapPD_j \subseteq \mathbb{R}_{\geq 0}, CapES_j \subseteq \mathbb{R}_{\geq 0} \quad \forall\, j \in J \tag{28}$$

$$PC_{j,h} \subseteq \mathbb{R}_{\geq 0}, PD_{j,h} \subseteq \mathbb{R}_{\geq 0}, SOC_{j,h} \subseteq \mathbb{R}_{\geq 0}, YS_{j,h} \in \{0,1\} \quad \forall\, h \in H, j \in J \tag{29}$$

ISO load, conventional generation data, and potential for energy storage

Data regarding load time series as well as power generation time series for nuclear, hydro, and other renewable power plants were collected for every ISO based on 2019 operational reports. In this work, we focus on the 2050 operation time frame; therefore, the 2019 load time series ($2019Load_h$) for each ISO was scaled up based on projected data by the U.S. Energy Information Administration[32], as described in equation 30. Parameter $2050TLoad$ denotes the projected total load for the corresponding ISO in 2050. On the other hand, power generation for nuclear, hydro, and other renewables is fixed based on the 2019 time series, as follows: $Nuclear_h = 2019Nuclear_h \; \forall\, h \in H$, $Hydro_h = 2019Hydro_h \; \forall\, h \in H$, and $OtherRen_h = 2019OtherRen_h \; \forall\, h \in H$, where parameters $2019Nuclear_h$, $2019Hydro_h$, and $2019OtherRen_h$ represent the 2019 power generation time series for nuclear, hydro, and other renewable power plants, respectively. Note that the nuclear and hydropower generation in United States is projected to decline in the 2019–2050 time frame, whereas biomass power generation is projected to increase[32]. Moreover, there is flexibility in hydro, biomass, and geothermal power generation that we are not considering. Adjusting

the behavior of these renewable units can also mitigate the need for some storage, but it is unlikely to affect the overall results and trends.

The corresponding load and power generation time series used by SDOM are provided in the Supplementary Figs. 2-8. Regarding the potential for energy storage, we allow for the installation of any energy capacity for each generic storage technology in each ISO. Note that this assumption requires a more detailed analysis of the potential for technologies like PHS, CAES, and hydrogen storage in each ISO's territory, which is out of the scope of this study.

$$Load_h = \frac{2050TLoad}{\sum_{h\in H} 2019TLoad_h} \cdot 2019Load_h \quad \forall\, h \in H \qquad 30$$

VRE capacity, representative profiles, and transmission cost

We used the reV model[33] to estimate the maximum available capacities, required transmission investments, and representative generation profiles (with hourly resolution) for each ISO and for a 1-year optimization window. Specifically, we used reV to generate time-synchronous solar PV and wind generation profiles based on 2012 weather data. reV uses resource assessment cells of 2 km x 2 km for wind and 4 km x 4 km for solar PV, which are aggregated into a maximum area of 33.2 km^2 considering spatial exclusions—i.e., the developable area is 33.2 km^2 minus excluded areas. These exclusions can be classified into: (i) regulatory restrictions (local, state, or federal protected land, urban and suburban areas, and protected wildlife species habitat), (ii) technical barriers (steep terrain and water bodies), and (iii) stakeholder constraints (U.S. Department of Defense lands, U.S. Forest Service lands, and private conservation areas)[33]. Thus, this spatial granularity allows for a better representation of differences in VRE siting and generation profiles, land-use restrictions, and transmission capacity required to integrate a given VRE facility. Note that the spatial resolution feature of SDOM refers to the spatial modeling of VRE generation. For solar PV, the selected technology is 1-axis tracking utility-scale solar PV with a ratio of direct current (DC) to alternating current (AC) of 1.3, tilt angle of 0°, azimuth of 180°, power density of 32 MW per km^2, and ground cover ratio of 0.4[33]. For land-based wind, different technologies or classes—e.g., from Class 1 to Class 10—can be selected for each location based on the average wind speed (meter per second) as defined by NREL's 2020 Annual Technology Baseline[33,36] and using a power density of 3 MW per km^2. Representative capacity factor time series are generated based on the weighted average approach. Additionally, required transmission investment or cost is calculated for each VRE location based on the distance to the interconnection point, a line cost of US$3,777.7 per MW-mile, and a line tie-in cost of US$14,422.5 per MW (if required)[33]. The total number of potential solar PV facilities varies from 2,000 to 3,000, depending on the ISO, whereas the total number of potential wind facilities varies from 3,477 to 6,000. A summary of the maximum power generation capacity and the yearly average capacity factor for each ISO is presented in Supplementary Figs. 9–15.

Metrics for VRE and energy storage deployment and operation

To analyze the results from SDOM, we define some metrics for the optimal deployment of VRE generation capacity and the storage portfolio. First, the VRE share ($VREshare$ (%)) is calculated using equation 31, and VRE curtailment ($VREcurtailment$ (%)) is evaluated via equation 32. Finally, the installed VRE generation capacity ($VREcapacity$) is calculated using equation 33.

$$VREshare = 100 \cdot \sum_{h \in H} \left(\frac{GenSolar_h + GenWind_h}{Load_h + \sum_{j \in J} (PC_{j,h} - PD_{j,h})} \right) \quad 31$$

$$VREcurtailment = 100 \cdot \sum_{h \in H} \left(\frac{CurtSolar_h + CurtWind_h}{GenSolar_h + CurtSolar_h + GenWind_h + CurtWind_h} \right) \quad 32$$

$$VREcapacity = \sum_{k \in K} CapSolar_k \cdot YSolar_k + \sum_{w \in W} CapWind_w \cdot YWind_w \quad 33$$

The storage discharge duration for each technology ($Sduration_j$) is calculated based on equation 34. The normalized SOC ($nSOC_{j,h}$) for storage technologies is calculated using equation 35. Additionally, total storage power capacity ($STPcapacity$) and total storage energy capacity ($STEcapacity$) are calculated based on equations 36 and 37, respectively. Finally, the average residual load ($AVRload$) is calculated using equation 38 and is based on the total number of hours considered in the optimization window ($|H|$).

$$Sduration_j = \frac{\sqrt{\eta_j} \cdot CapES_j}{CapPD_j} \quad \forall\, j \in J \quad 34$$

$$nSOC_{j,h} = \frac{SOC_{j,h}}{CapES_j} \quad \forall\, h \in H, j \in J \quad 35$$

$$STPcapacity = \left(\frac{1}{2}\right) \cdot \sum_{j \in J} (CapPC_j + CapPD_j) \quad 36$$

$$STEcapacity = \sum_{j \in J} CapES_j \quad 37$$

$$AVRload = \frac{\sum_{h \in H} (Load_h - \alpha_{nuclear} \cdot Nuclear_h - Hydro_h - OtherRen_h)}{|H|} \quad 38$$

Storage cycling is measured using equivalent cycles, which represent a sum of storage charging power for a specific technology with respect to the total energy storage capacity of that technology. Equivalent discharge cycles are calculated using equation 39.

$$EquivalentDischargeCycles_j = \frac{\sum_{h \in H} PD_{j,h}}{CapES_j} \quad \forall\ j\ \in J \tag{39}$$

The average electricity supply cost or energy cost ($Energycost$ ($US\$\ per\ MWh$)) is calculated using equation 40. Moreover, the cost of avoided CO_2 emissions is calculated based on the fuel emission factor ($CO2Emi$) (tonnes of CO_2 per MMBtu) and the heat rate ($HRbu$) of the balancing unit, as described in equation 41. Parameters $TSCref$ and $GenBUref_h$ denote the total system cost and the hourly generation from the balancing unit for the reference case, respectively. The reference case corresponds to the optimal power system design without enforcing any target for carbon-free or renewable energy mix—i.e., removing equation 7 from the mathematical formulation.

$$Energycost = \frac{TSC}{\sum_{h \in H}(Load_h - \alpha_{nuclear}.Nuclear_h - Hydro_h - OtherRen_h)} \tag{40}$$

$$CostCO2 = \frac{TSC - TSCref}{CO2Emi \cdot HRbu \cdot \sum_{h \in H}(GenBUref_h - GenBU_h)} \tag{41}$$

Soft link of SDOM to long-term and large-scale energy planning and operation models

Despite recent progress on the techno-economic modeling of energy storage[45], modeling of energy storage—particularly for long-duration and seasonal applications—in long-term and large-scale energy planning and operation models remains a major challenge[46]. On the other hand, storage modeling tools, e.g., price-taker or copperplate tools, do not accurately represent power system details. For instance, SDOM assumes no transmission constraints, perfect foresight of electricity demand and VRE generation, and no power import/export with neighboring regions. In this section, we speculate on how SDOM and the framework established in this paper could be used to improve the modeling of storage technologies in long-term and large-scale power capacity planning and production cost models. Power capacity planning models are used to optimize long-term expansion—based on a multidecadal time window—of generation and transmission power capacity. These models usually have lower temporal and spatial resolutions but wider geographic coverage than production cost models used for power systems operations optimization. For instance, power capacity planning models could be based on time slices or representative days and balancing areas with a limited representation of the chronology of operational

decisions, which is critical to accurately model storage technologies of any discharge duration.

In contrast, production cost models are used to assess system operations by optimizing unit commitment and economic dispatch decisions based on exogenous power generation and transmission build-out and require higher temporal and spatial resolutions. For example, production cost models could use hourly resolution and nodal modeling of the transmission network, allowing for a better representation of the chronology of operational decisions; however, production cost models are usually run with a short optimization window (e.g., 1 day), and they are run sequentially because of the computational challenges of optimizing the hourly operation for the entire year. Thus, the optimization of long-duration and seasonal energy storage in production cost models is challenging. In this context, SDOM can provide information regarding the scale of storage requirements—e.g., power capacity and discharge duration—and operational policies for short-duration, long-duration, and seasonal storage technologies. For power capacity planning models, results from SDOM can be used to define the operational profile of storage devices as well as the scale of the associated power and energy capacities. Note that the power capacity planning model could be allowed to adjust these capacities based on just one or multiple devices for each storage technology. In summary, SDOM can be used to prescreen energy storage requirements and inputs for the power capacity planning model. Moreover, the production cost model can leverage SDOM to simulate long-duration and seasonal storage technologies based on the spatially distributed power and energy capacity deployment provided by the capacity planning model and the operational policies provided by SDOM.

Acknowledgments

This work was authored in part by the National Renewable Energy Laboratory, operated by Alliance for Sustainable Energy, LLC, for the U.S. Department of Energy (DOE) under Contract No. DE-AC36-08GO28308. Funding provided by U.S. Department of Energy Office of Energy Efficiency and Renewable Energy Office of Strategic Programs and Fuel Cell Technologies Office. The views expressed in the article do not necessarily represent the views of the DOE or the U.S. Government. The U.S. Government retains and the publisher, by accepting the article for publication, acknowledges that the U.S. Government retains a nonexclusive, paid-up, irrevocable, worldwide license to publish or reproduce the published form of this work, or allow others to do so, for U.S. Government purposes.

References

1. International Energy Agency. *Status of Power System Transformation 2019: Power system flexibility*. *OECD Publishing* (OECD, 2019). doi:10.1787/7c49400a-en

2. IRENA. *Planning for the renewable future: Long-term modelling and tools to expand variable renewable power in emerging economies*. (2017).

3. Kroposki, B. *et al.* Achieving a 100% Renewable Grid: Operating Electric Power Systems with Extremely High Levels of Variable Renewable Energy. *IEEE Power Energy Mag.* **15**, 61–73 (2017).

4. Lund, P. D., Lindgren, J., Mikkola, J. & Salpakari, J. Review of energy system flexibility measures to enable high levels of variable renewable electricity. *Renew. Sustain. Energy Rev.* **45**, 785–807 (2015).

5. Beaudin, M., Zareipour, H., Schellenberglabe, A. & Rosehart, W. Energy storage for mitigating the variability of renewable electricity sources: An updated review. *Energy Sustain. Dev.* **14**, 302–314 (2010).

6. Luo, X., Wang, J., Dooner, M. & Clarke, J. Overview of current development in electrical energy storage technologies and the application potential in power system operation. *Appl. Energy* **137**, 511–536 (2015).

7. Guerra, O. J. Beyond short-duration energy storage. *Nat. Energy* **6**, 460–461 (2021).

8. Braff, W. A., Mueller, J. M. & Trancik, J. E. Value of storage technologies for wind and solar energy. *Nat. Clim. Chang.* **6**, 964–969 (2016).

9. Mallapragada, D. S., Sepulveda, N. A. & Jenkins, J. D. Long-run system value of battery energy storage in future grids with increasing wind and solar generation. *Appl. Energy* **275**, 115390 (2020).

10. The Advanced Research Projects Agency- Energy (ARPA-E). Duration Addition to electricitY Storage (DAYS) Overview. 1–12 (2018). Available at: https://arpa-e.energy.gov/?q=arpa-e-programs/days.

11. Albertus, P., Manser, J. S. & Litzelman, S. Long-Duration Electricity Storage Applications, Economics, and Technologies. *Joule* **4**, 21–32 (2020).

12. Dowling, J. A. *et al.* Role of Long-Duration Energy Storage in Variable Renewable Electricity Systems. *Joule* 1–22 (2020). doi:10.1016/j.joule.2020.07.007

13. Sepulveda, N. A., Jenkins, J. D., Edington, A., Mallapragada, D. S. & Lester, R. K. The design space for long-duration energy storage in decarbonized power systems. *Nat. Energy* (2021). doi:10.1038/s41560-021-00796-8

14. Guerra, O. J. *et al.* The value of seasonal energy storage technologies for the integration of wind and solar power. *Energy Environ. Sci.* **13**, 1909–1922 (2020).

15. Hunter, C. A. *et al.* Techno-economic analysis of long-duration energy storage and flexible power generation technologies to support high-variable renewable energy grids. *Joule* 1–25 (2021). doi:10.1016/j.joule.2021.06.018

16. Cebulla, F., Naegler, T. & Pohl, M. Electrical energy storage in highly renewable European energy systems: Capacity requirements, spatial distribution, and storage dispatch. *J. Energy Storage* **14**, 211–223 (2017).

17. Frew, B. A., Becker, S., Dvorak, M. J., Andresen, G. B. & Jacobson, M. Z. Flexibility mechanisms and pathways to a highly renewable US electricity future. *Energy* **101**,

65–78 (2016).

18. Dunn, B., Kamath, H. & Tarascon, J.-M. Electrical Energy Storage for the Grid: A Battery of Choices. *Science* **334**, 928–935 (2011).

19. Yang, Z. *et al.* Electrochemical Energy Storage for Green Grid. *Chem. Rev.* **111**, 3577–3613 (2011).

20. Gür, T. M. Review of electrical energy storage technologies, materials and systems: challenges and prospects for large-scale grid storage. *Energy Environ. Sci.* **11**, 2696–2767 (2018).

21. Zakeri, B. & Syri, S. Electrical energy storage systems: A comparative life cycle cost analysis. *Renew. Sustain. Energy Rev.* **42**, 569–596 (2015).

22. Schmidt, O., Melchior, S., Hawkes, A. & Staffell, I. Projecting the Future Levelized Cost of Electricity Storage Technologies. *Joule* **3**, 81–100 (2019).

23. Poonpun, P. & Jewell, W. T. Analysis of the Cost per Kilowatt Hour to Store Electricity. *IEEE Trans. Energy Convers.* **23**, 529–534 (2008).

24. Balducci, P. J., Alam, M. J. E., Hardy, T. D. & Wu, D. Assigning value to energy storage systems at multiple points in an electrical grid. *Energy Environ. Sci.* **11**, 1926–1944 (2018).

25. Xu, B. *et al.* Scalable Planning for Energy Storage in Energy and Reserve Markets. *IEEE Trans. Power Syst.* **32**, 4515–4527 (2017).

26. Denholm, P. *et al. The Value of Energy Storage for Grid Applications*. (National Renewable Energy Laboratory (NREL), 2013). doi:10.2172/1220050

27. Cebulla, F., Haas, J., Eichman, J., Nowak, W. & Mancarella, P. How much electrical energy storage do we need? A synthesis for the U.S., Europe, and Germany. *J. Clean. Prod.* **181**, 449–459 (2018).

28. Budischak, C. *et al.* Cost-minimized combinations of wind power, solar power and electrochemical storage, powering the grid up to 99.9% of the time. *J. Power Sources* **225**, 60–74 (2013).

29. Mileva, A., Johnston, J., Nelson, J. H. & Kammen, D. M. Power system balancing for deep decarbonization of the electricity sector. *Appl. Energy* **162**, 1001–1009 (2016).

30. Zeyringer, M., Price, J., Fais, B., Li, P.-H. & Sharp, E. Designing low-carbon power systems for Great Britain in 2050 that are robust to the spatiotemporal and inter-annual variability of weather. *Nat. Energy* **3**, 395–403 (2018).

31. Shaner, M. R., Davis, S. J., Lewis, N. S. & Caldeira, K. Geophysical constraints on the reliability of solar and wind power in the United States. *Energy Environ. Sci.* **11**, 914–925 (2018).

32. U.S. Energy Information Administration. Annual Energy Outlook 2020 (AEO2020). Available at: https://www.eia.gov/outlooks/aeo/tables_ref.php. (Accessed: 12th

October 2020)

33. Maclaurin, G. J., Grue, N. W., Lopez, A. J. & Heimiller, D. M. *The Renewable Energy Potential (reV) Model: A Geospatial Platform for Technical Potential and Supply Curve Modeling*. (2019). doi:10.2172/1563140

34. Mongird, K. *et al.* 2020 Grid Energy Storage Technology Cost and Performance Assessment. 117 (2020).

35. Ziegler, M. S. *et al.* Storage Requirements and Costs of Shaping Renewable Energy Toward Grid Decarbonization. *Joule* **3**, 2134–2153 (2019).

36. National Renewable Energy Laboratory. 2020 Annual Technology Baseline (ATB). (2020). Available at: https://atb.nrel.gov/electricity/2020/data.php. (Accessed: 12th October 2020)

37. Millstein, D., Wiser, R., Bolinger, M. & Barbose, G. The climate and air-quality benefits of wind and solar power in the United States. *Nat. Energy* **2**, 17134 (2017).

38. Weitemeyer, S., Kleinhans, D., Vogt, T. & Agert, C. Integration of Renewable Energy Sources in future power systems: The role of storage. *Renew. Energy* **75**, 14–20 (2015).

39. Hunt, J. D. *et al.* Global resource potential of seasonal pumped hydropower storage for energy and water storage. *Nat. Commun.* **11**, 947 (2020).

40. Aghahosseini, A. & Breyer, C. Assessment of geological resource potential for compressed air energy storage in global electricity supply. *Energy Convers. Manag.* **169**, 161–173 (2018).

41. Lord, A. S., Kobos, P. H. & Borns, D. J. Geologic storage of hydrogen: Scaling up to meet city transportation demands. *Int. J. Hydrogen Energy* **39**, 15570–15582 (2014).

42. Mongird, K. *et al. Energy Storage Technology and Cost Characterization Report*. (2019). doi:10.2172/1573487

43. General Algebraic Modeling System (GAMS). Available at: https://www.gams.com/.

44. CPLEX. Available at: https://www.gams.com/latest/docs/S_CPLEX.html.

45. Hittinger, E. & Ciez, R. E. Modeling Costs and Benefits of Energy Storage Systems. *Annu. Rev. Environ. Resour.* **45**, (2020).

46. Bistline, J. *et al.* Energy storage in long-term system models: a review of considerations, best practices, and research needs. *Prog. Energy* **2**, 1–22 (2020).